Radial Response of Outer Radiation Belt Relativistic Electrons During Enhancement Events at Geostationary Orbit

Victor A. Pinto[1], Jacob Bortnik[1], Pablo. S. Moya[2], Larry R. Lyons[1], David G. Sibeck[3], Shrikanth G. Kanekal[3], Harlan E. Spence[4], Daniel N. Baker[5]

[1]Department of Atmospheric and Oceanic Sciences, University of California, Los Angeles, CA, USA.
[2]Departamento de Física, Facultad de Ciencias, Universidad de Chile, Santiago, Chile.
[3]NASA Goddard Space Flight Center, Heliophysics Science Division, Greenbelt, MD, USA.
[4]Institute for the Study of Earth, Oceans, and Space, University of New Hampshire Durham, New Hampshire, USA
[5]Laboratory for Atmospheric and Space Physics, University of Colorado Boulder, Boulder, CO, USA.

Key Points:

- The radial response of the outer radiation belt during relativistic electron enhancements at geostationary orbit is characterized
- Enhancements at GEO generally penetrate to $L = 5.0$ but at lower L they may respond differently and even be seen as depletions
- Geomagnetic indices, especially AE and $D_{\rm st}$ show a remarkable capacity to determine lowest $L-$shell of enhancement

Corresponding author: Victor A. Pinto, `victor.pinto@gmail.com`

Abstract

Forecasting relativistic electron fluxes at geostationary Earth orbit (GEO) has been a long term goal of the scientific community, and significant advances have been made in the past, but the relation to the interior of the radiation belts, that is, to lower $L-$shells is still not clear. In this work we have identified 60 relativistic electron enhancement events at GEO to study the radial response of outer belt fluxes and the correlation between the fluxes at GEO and those at lower $L-$shells. The enhancement events occurred between 1 October 2012 and 31 December 2017 and were identified using GOES 15 >2 MeV fluxes at GEO, which we have used to characterize the radial response of the radiation belt, by comparing to fluxes measured by the Van Allen probes ECT-REPT between $2.5 < L < 6.0$ at $E = 2.1$ MeV. We have found that in general the response of the radiation belts during enhancement events is cohesive for $L > 5.0$, and generally similar for $L > 4.5$. Post enhancement maximum fluxes show a remarkable correlation for all $L > 4.0$ although the magnitude of the pre-existing fluxes on the outer belt plays a significant role and makes the ratio of pre-to-post enhancement fluxes less predictable in the region $4.0 < L < 4.5$. For $L < 4$ the fluxes are poorly correlated with geostationary orbit, but they also tend to be less variable. We have also examined SYM-H, Kp and AE indices and found that depending on their magnitude, the response of different parts of the outer belt can be better quantified.

1 Introduction

The Earth's outer radiation belt, located approximately in the region between $3 < R_E < 7$ consists mostly of trapped electrons with energies ranging from few tens of keV up to tens of MeV. These electron populations are very dynamic and fluxes are known to vary by several orders of magnitude in periods of time ranging from hours to days (e.g. X. Li et al., 1999; Millan & Thorne, 2007; Thorne, 2010; Thorne et al., 2013; Jaynes et al., 2015). Such extreme responses are known to be associated with changes in the solar wind (Paulikas & Blake, 1979; Reeves et al., 2011), the phase of the solar cycle (Baker et al., 1986) and increased levels of geomagnetic activity (Reeves, 1998). Geomagnetic storms have been the centerpiece of the investigation of enhancements of relativistic electrons as they are known to provide the necessary energy input into the system to set the inner magnetosphere in motion. Yet, Reeves et al. (2003) found that only around 50% of geomagnetic storms result in enhancement of fluxes at geostationary orbit since loss processes are enhanced together with acceleration processes during storm periods. It has been shown that geomagnetic storms, defined by a significant drop in the D_{st} index (Gonzalez et al., 1994), are not required to produce enhancement events (Anderson et al., 2015; Schiller et al., 2014; Kim et al., 2015; Pinto et al., 2018; Su et al., 2014) since energy transfer mechanisms that are not efficient at driving enhancements in the ring current, and hence the D_{st} index, can still provide the required energy for enhancement of electron fluxes (Borovsky & Denton, 2010; Denton & Borovsky, 2012).

In the past, the bulk of studies focused on enhancement of relativistic electrons at geostationary Earth orbit (GEO). Located at $R_E \sim 6.6$, the geostationary orbit is a key location for communication and meteorological satellites, and therefore has provided scientific measurements of the outer radiation belt for several decades. Due to its location in the outer part of the radiation belt, dramatic changes can occur in electron fluxes. Since relativistic ($\sim$MeV) electrons that get enhanced can cause malfunctions in satellite equipment (Baker, 2000; G. L. Wrenn et al., 2002; G. Wrenn, 2009), many efforts have been made to understand what causes enhancements at GEO (O'Brien et al., 2001; Hajra et al., 2015; Kim et al., 2006, 2015; Balikhin et al., 2011; Lyatsky & Khazanov, 2008; Iles et al., 2002) as well as to accurately forecast their behavior (Baker et al., 1990; X. Li et al., 2001; Turner & Li, 2008; Simms et al., 2014, 2016; Boynton et al., 2015).

The launch of the Van Allen Probes mission in 2012 provided a unique opportunity to expand studies of relativistic electron enhancements to the whole extent of the outer radiation belt (Mauk et al., 2013). The response of the outer radiation belt to geomagnetic storms has been studied in detail for relativistic (e.g. Turner et al., 2015) and ultrarelativistic (i.e. $\gamma > 10$) energies (e.g. Moya et al., 2017; Xiong et al., 2015, 2018; Zhao et al., 2019; Katsavrias et al., 2019; Tang et al., 2017; Murphy et al., 2018), and their dependence on the solar wind driver of the storms (e.g. Pandya et al., 2019; Bingham et al., 2018; Yuan & Zong, 2019; W. Li et al., 2015; Shen et al., 2017). Recently, Turner et al. (2019) presented an extended overview of the state of the response of the electron radiation belt to geomagnetic storms summarizing most of the findings during the Van Allen Probes era and showing that storm-time response of the radiation belt is qualitatively predictable.

Several models of different kinds have been developed to forecast the state of the outer radiation belt based on the real-time measurements of the Van Allen Probes. However, the end of the mission requires the development of forecast methods that rely on proxy measurements. Although several attempts have been made with low-orbiting satellites, in this study we take a different approach and explore the use of geostationary data from the GOES satellites as a possible proxy for the state of the outer radiation belt. Recently, Baker et al. (2019) has calculated the correlation between daily averaged fluxes at geostationary orbit and the Van Allen Probes mission, establishing a baseline statistics for how often we should expect to be able to use the GEO boundary as a predictor for fluxes at lower L-shells. Additionally, Moya et al. (2017) showed that when geomagnetic storms result in enhancement of fluxes, there is a relatively coherent response of the belt for $L > 4.5$. In this paper we focus on the relativistic electron enhancement events at GEO and determine under which circumstances the correlation to fluxes at lower $L-$shells, and therefore the potential for forecast across the whole outer belt, can be improved. This paper is presented as follows. Section 2 describes the data utilized and the event selection criteria. In section 3 we compare the response of the fluxes from GOES and Van Allen Probes for 60 events that occurred between 1 October 2012 and 31 December 2017. Section 4 we study the correlation between fluxes at GEO and those at different $L-$shells. In section 5 we study magnetospheric parameters associated with those events to estimate to what extent we can use GEO data from GOES satellites to estimate the fluxes of relativistic electrons across the outer radiation belts and what are the current limitations. Finally, in section 6 we summarize and discuss the findings of this study.

2 Data and Events

Relativistic electron enhancement (REE) events at GEO are defined as prolonged periods of time over which electron fluxes recover from a dropout and exceed a minimum threshold, for example, NOAA issues warnings when $f_{\mathrm{GEO}} > 10^3$ cm^{-2} sr^{-1} s^{-1}. Here we follow the definition used in Pinto et al. (2018) and Kim et al. (2006) that defines an enhancement event as an increase in electron fluxes from less than 10^2 cm^{-2} sr^{-1} s^{-1} to more than $2{\times}10^3$ cm^{-2} sr^{-1} s^{-1} in less than 2 days, and maintains an average daily flux larger than 10^3 cm^{-2} sr^{-1} s^{-1} for at least 3 days. The increase by at least an order of magnitude in fluxes, as well as the relatively long 3-day interval of elevated fluxes attempts to avoid confusion between real increases in flux, and purely adiabatic effects which are reversible and recover when D_{st} recovers (Kim & Chan, 1997). To identify REE events we used > 2 MeV electron fluxes obtained from the Geostationary Operational Environmental Satellite (GOES) 15 Energetic Proton, Electron and Alpha Detector (EPEAD) instrument (Rodriguez et al., 2014), sampled at 5 minute temporal resolution. From 1 September 2012 to 31 December 2017 we found 60 REE events at GEO. For each event, we have determined a time $t = 0$ as the last time before the general trend of increase in fluxes is detected, given that $-1 < t < 0$ days define the minimum daily average flux of the period of study, and that the daily average flux for $t > 0$ continually increases in the next 2-3 days until the enhancement flux threshold has been met. This selection of a time $t = 0$ is different from the more traditionally used time of minimum D_{st} (or SYM-H) (e.g. O'Brien et al., 2001) and reflects the assumption that we do not consider geomagnetic storms to be a strict requirement in the search of REE events, but the two phenomena are both results of the same driving conditions. Indeed, a geomagnetic storm defined by a minimum $D_{\mathrm{st}} < -50$ nT (Gonzalez et al., 1994) has long been shown to be not strictly required for the occurrence of REE events at GEO (Kim et al., 2015; Pinto et al., 2018; Hajra et al., 2015; Anderson et al., 2015; Su et al., 2014; Schiller et al., 2014). This is explained in part by the fact that a significant number of events are associated with a high-speed stream driven Corrotational Interaction Region (CIR), which has been shown to be effective at driving REE's but can be less effective at causing D_{st} drops (Borovsky & Denton, 2006, 2010). A detailed list of the dates of each event with their respective solar wind driver, maximum Kp index and $SYM - H$ minimum values can be found in the supporting information.

To study the response of the outer electron radiation belt as a function of $L-$shell during REEs at GEO, we used data from the Van Allen Probes (Mauk et al., 2013) Energetic Particle, Composition and Thermal Plasma Suite (Spence et al., 2013) Relativistic Electron-Proton Telescope (Baker et al., 2013) (ECT-REPT). As we want to compare between GOES and the Van Allen Probes, we will use the $E = 2.1$ MeV differential energy channel. The data has been processed following a procedure similar to the one described in Moya et al. (2017), that is, we have calculated omni-directional fluxes by averaging over all pitch angles, and then we have performed a binning to $\Delta L = 0.1$. We then combined data from RBSP-A and RBSP-B and performed a new binning in both time $\Delta t = 6$ hours and space $\Delta L = 0.1$. This procedure ensures continuous coverage over all $2.5 < L < 6.0$ but reduces the temporal resolution to 4 points a day. To determine enhancements in the outer belt during each event, we follow the more traditional definition of evaluating whether the maximum fluxes in the time interval $12 < t < 96$ hours ($t = 0$ is defined by the GOES events) are at least twice the maximum fluxes during the interval $-72 < t - 12$ hours for every $L-$shell between $2.5 < L < 6.0$ (Reeves et al., 2003; Turner et al., 2015; Moya et al., 2017). To avoid spurious results due to oscillations in low fluxes, we also require that the maximum flux after $t = 0$ for a particular $L-$shell to be larger than the 25 percentile values calculated from the entire Van Allen Probes mission (values can be found in the supporting information).

Figure 1 shows the temporal evolution of two different REE events that occurred on 08 October 2012 (left) and 13 May 2015 (right). Both events are associated with large geomagnetic storms (SYM-H min ~ -100 nT), continuously elevated AE index values for at least one day after $t = 0$, large $>$ 500 km/s solar wind speed and a somewhat negative interplanetary magnetic field B_z. Differences do exist in maximum V_x and soutward IMF B_z intensity, but despite these differences both events result in very similar maximum flux values as observed at GEO of $\sim 2 \times 10^4$ cm^{-2} sr^{-1} s^{-1} during the recovery phase of the storm and on the following days. These similarities in flux evolution at GEO are still present down to $L = 5.5$ but do not propagate inward across the rest of the outer radiation belts. Panels (b) and (h) show the $E = 2.1$ MeV channel as a function of $L-$shell. The black lines correspond to the contours of 90% and 75% of the maximum log(flux) illustrating the differences in penetration to lower $L-$shells. It can

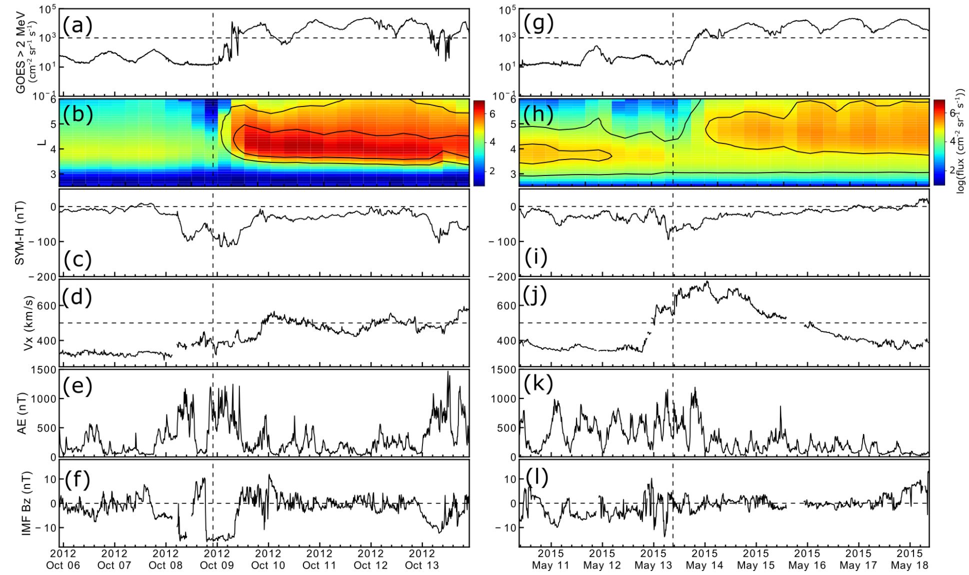

Figure 1. Two relativistic electron enhancement (REE) events that occurred on 08 October 2012 (left) and 13 May 2015 (right). From top to bottom: (a,g) > 2 MeV electron flux from GOES 15, (b,h) Van Allen Probes REPT $E = 2.1$ MeV electron flux binned in time and space. Contours correspond to 90% and 75% of log(maximum flux) showing the different regions of maximum enhancement. Lower panels show SYM-H index (c,i), solar wind speed (d,j) , AE index (e, k) and interplanetary magnetic field B_z component (f,l).

be appreciated from the figure that the event of 08 October 2012 presents significant enhancement down to $L \sim 3.2$ with a peak in flux at $L = 4.0$. The event of 13 May 2015 shows an enhancement down to $L \sim 4.0$ with peaks in fluxes at $L = 4.5$ More importantly, the enhancement profiles are very different, fluxes for the event of 08 October 2012 are up to an order of magnitude larger than in the event of 13 May 2015 in the region $3.5 < L < 5.0$ but are actually lower in the region $L < 3.3$. Still the high magnitude of pre-existing fluxes on the belt results in a depletion (when comparing by L) of fluxes for the 13 May 2015 events for all $L < 3.7$.

The examples in Figure 1 show that REE events that look similar at GEO may respond very differently at different L-shells across the outer radiation belt, and especially so at lower $L-$shells. Also, the magnitude of pre-existing fluxes on the belt may play an important role in the interpretation of any statistical analysis that uses ratios of post-to-pre enhancement fluxes and therefore must be considered. In the following sections we characterize the similarities and differences in the response of the belt as a function of L for the 60 events we have found and quantify how the strength of some geomagnetic indices translates to predictive capabilities of the extent of the enhancements across the outer belt.

3 Radial response of relativistic electron enhancement events

To understand the evolution of the outer radiation belt at different $L-$shells we have estimated the ratio of change in electron fluxes for all $2.5 < L < 6.0$. Figure 2 shows the comparison of the maximum fluxes measured in the $-72 < t < -12$ hours prior to $t = 0$ and maximum fluxes measured in the $12 < t < 96$ hours after $t = 0$. The different panels show electron fluxes at GEO and at 7 different $L-$shells ranging from $L = 6.0$ and decreasing at intervals of $\Delta L = 0.5$ to $L = 3.0$. Blue (red) dashed lines in each panels correspond to a ratio $r = 2.0$ ($r = 0.5$), traditionally used to determine an enhancement (depletion) event (e.g. Reeves et al., 2003). Individual events have been color-coded following the same definition.

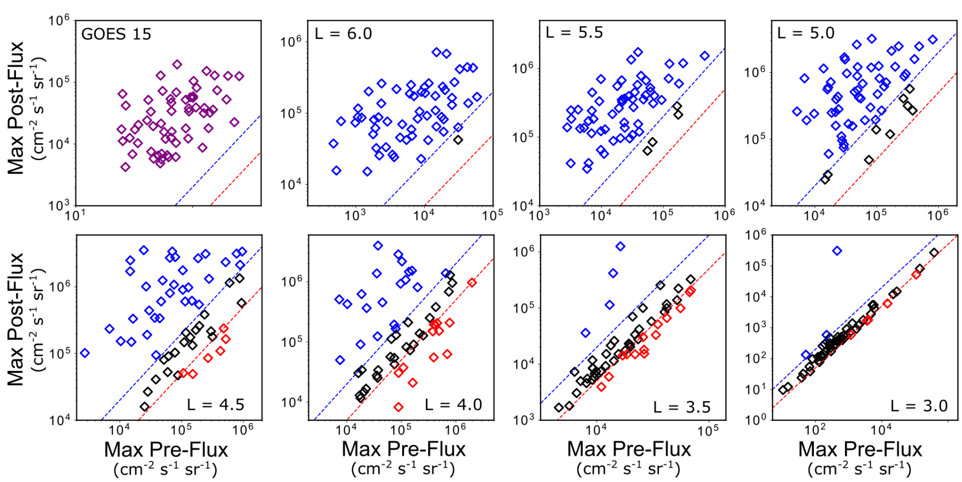

Figure 2. Maximum post-to-pre $t = 0$ fluxes at geostationary orbit (GOES 15) and at different $L-$shells from Van Allen Probes data. Dashed blue (red) lines mark the ratio $r = 2.0$ (r=0.5). Individual events have been color coded according to whether their ratio is indicative of an increase $r > 2.0$ (blue), a decrease $r < 0.5$ (red) or in between showing no change (black).

Figure 2 shows the drastic decrease in the effectiveness of the enhancement response as $L-$shell decreases. At $L = 6.0$, all but one event (98%) result in enhancements, which decreases to 85% at $L = 5.0$. However, for $L < 5.0$ the decrease in occurrence is significant, with only 36% of events resulting in enhancement of fluxes at $L = 4.0$ and only

5% at $L = 3.0$. Since Figure 2 also shows the changes in fluxes, we can notice that the trend is to move towards lower post-to-pre flux ratios as we move to lower $L-$shells. Several events present little to no change ($0.5 \leq r \leq 2.0$) for $L \leq 5.0$ which then becomes the majority of the events at $L = 3.0$. Additionally, a number of events correspond to depletions ($r < 0.5$) between $3.0 < L < 4.5$, with a peak in the decrease in fluxes at $L = 4.0$ where the depletions appear to be most significant suggestive of a possible local loss mechanism (e.g. Bortnik et al., 2006; Mourenas et al., 2016; Blum & Breneman, 2019).

Figure 3 expands the information of Figure 2 to all $L-$shells in the range $2.5 \leq L \leq 6.0$. Figure 3(a) shows the occurrence (in percentage) of enhancements, depletions and no-change of fluxes as a function of $L-$shell. Between $6.0 < L < 5.1$ the occurrence of enhancement events is $> 90\%$ as would be expected since they are selected based on REEs at GEO. However, a significant decrease in enhancement occurrence takes place between $3.5 < L < 5.1$, decreasing down to only 8% of events resulting in enhancement of fluxes at $L = 3.1$. The number of unaffected (no change) events increase from 2% at $L = 6.0$ up to 98% at $L = 2.5$, indicating the range of effectiveness of propagating an REE from GEO towards the inner magnetosphere, the exception being the 17 March 2015 storm (minimum Dst $= -223$ nT) that caused an enhancement for all $L \geq 2.5$, consistent with the expected result that only extremely strong geomagnetic activity can affect the innermost part of the outer radiation belt. For $L < 4.7$ there are a number of events that present a depletion compared to pre $t = 0$ fluxes ($r < 0.5$). The peak occurrence of depletions is $\sim 25\%$ of events, which occurs at $3.4 < L < 3.8$, suggestive of a local loss mechanism.

Figure 3(b) shows the distribution of post-to-pre flux ratios as a function of $L-$shell for all 60 events. The black dots represent the median of the distribution at each $L-$shell; the green colored bars indicate the upper and lower quartiles of the distribution and black bars the 5th and 95 percentiles. The blue (red) dashed lines represent the enhancement (depletion) thresholds $r = 2.0$ ($r = 0.5$). The median of the distributions show a decrease in the flux ratio as L decreases that reaches a minimum at around $L = 3.5$ and that slightly increases for $L < 3.5$ to reach a value of almost $r = 1$ at $L = 2.5$, indicating the range of penetration of a REE at GEO. By showing the 5th and 95th percentiles we can get a sense of how much spread there is in the distribution for all $L > 4.0$ with the highest variability between $4.0 \leq L \leq 4.5$. A sharp decrease in the spread for $L <$

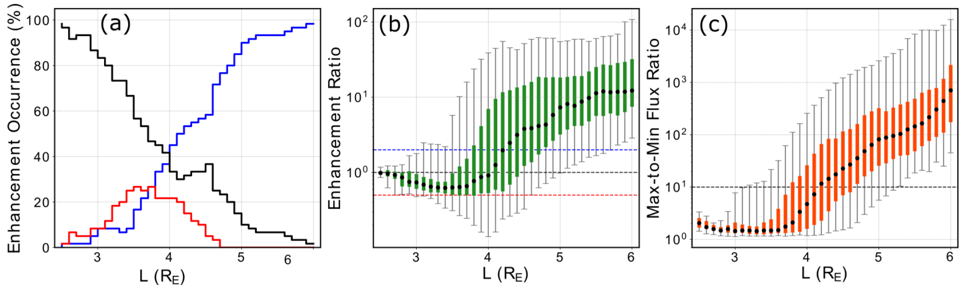

Figure 3. (a) Occurrence percentage as a function of L for enhancement (blue), depletion (red) and no-change (black) response of all 60 events. (b) Distribution of post-to-pre flux ratios as a function of $L-$shell. Black dots indicate median values, the colored bar corresponds to upper and lower quartile distributions and black lines indicate the 5th and 95th percentiles of the distribution of events at each $L-$shell. (c) Distribution of maximum to minimum flux ratio as a function of $L-$shell. Colored bars and black lines indicate similar percentiles as in (b).

3.5 indicates that this region is mostly unaffected by processes that affect the external part of the belt. The depletion zone $r < 0.5$ between $3.5 < L < 4.5$ indicates the region that is likely affected by the depletion processes driven by geomagnetic activity but not so much for the processes producing the enhancement of fluxes, for around 25% of the events and it shows that the peak in depletion occurrence is between $3.5 < L < 4.0$ with the strongest depletion rate at $L = 4.0$.

Figure 3(c) shows the distribution of the ratios of maximum flux post enhancement versus minimum flux measured within $-24 < t < 24$ hours, in the same format as Figure 3(b). The black dashed line is located at an increase in fluxes by a factor of 10 with respect to the minimum flux measured at that particular $L-$shell. At higher $L > 5.5$ the increase can be of 3-4 orders of magnitude with respect to the minimum measured flux but this factor also decreases as L decreases. For $L < 3.5$ the majority of the events presents no increase in fluxes with respect to the minimum value, and therefore the categorization of a depletion or a no-change event is mostly determined by the pre-existing magnitude of the fluxes and the dropout effectiveness at low $L-$shells instead of by any process occurring afterwards. Figure 3(b,c) also indicates that enhancements are less extreme as L decreases, although the maximum fluxes can be 1-2 orders of magnitude higher than at GEO.

4 Correlation of fluxes as a function of L

We have discussed the general response of the outer radiation belt during REE events at GEO. To get a better idea of the coherence of the response across the belt for all events, we have calculated the correlation coefficient between the fluxes at GEO and at different $L-$shells for three quantities of interest: the maximum flux post enhancement ($t > 0$), the maximum flux pre enhancement ($t < 0$)and the pre-to-post flux ratio. Figure 4 shows the correlation coefficient between the maximum fluxes post $t > 0$ at GEO and maximum fluxes at different $L-$shells every $\Delta L = 0.5$. The correlation coefficient is very high $R > 0.8$ for $L > 4.5$, indicating that the response of the outer belt at $L > 4.5$ is in general similar to the response that the geostationary orbit is experiencing. The correlation coefficient quickly decreases in the region $L < 4.5$ and becomes very low ($R < 0.2$) for $L < 3.0$ showing that in this region the response is independent to what occurs at higher altitude. Similar figures for the correlation coefficients of maximum flux pre enhancement and ratios can be found in the supporting information. Although they have a similar trend, they also show some significant differences.

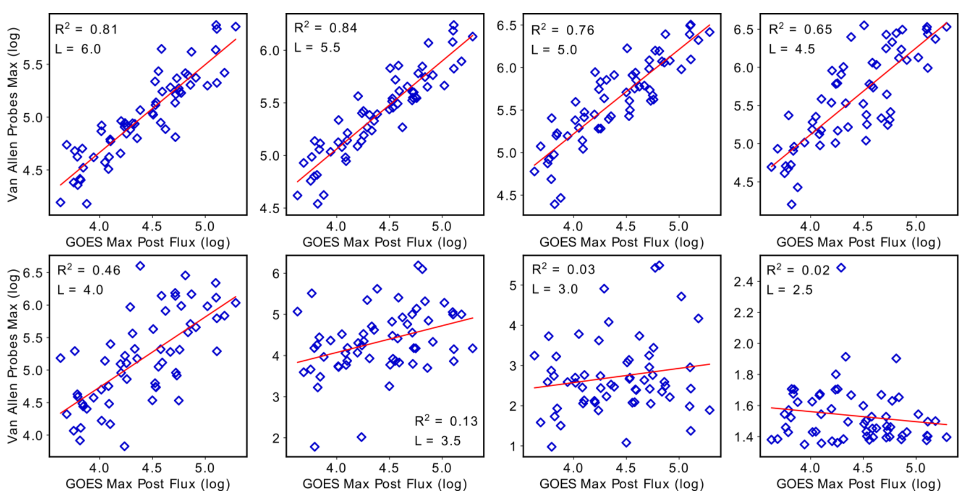

Figure 4. Maximum fluxes measured by GOES after $t = 0$ versus maximum fluxes measured by the Van Allen Probes at different $L-$shells. The red line indicates the best linear fit of the fluxes from which a correlation coefficient has been calculated, showing the general decrease in coherence as $L-$shell decreases.

Figure 5 shows the correlation coefficients obtained in Figure 4 as a function of $L-$shell, plus correlation coefficients calculated for maximum fluxes pre-enhancement and for the ratio maximum post-to-pre enhancement flux. The correlation coefficient is expected to increase and approach $R = 1$ as the measurements get closer together. Of course, the spatial gap between the Van Allen Probes and the GOES satellites ($\Delta L \geq 0.6$) plus the differences in the actual instruments (integrated channels in GOES versus differential energy channels in the Van Allen Probes), and calibrations can result in differences such that a perfect correlation is unlikely to be achieved. Still, for fluxes post enhancement the correlation coefficient is very high, peaking at $R = 0.94$ for $L = 5.8$. The slightly lower correlation coefficient at $L = 6.0$ is probably related to the lack of coverage from the Van Allen Probes during certain events since this L is larger than the radial distance of the spacecraft apogee, and thus requires data from off the equatorial plane, thus reducing accuracy relative to more equatorial measurements. The strong correlation for $L > 4.5$ and in particular for $L > 5.5$ confirms that by simply predicting the same flux evolution in this region as in GEO should have a very high accuracy.

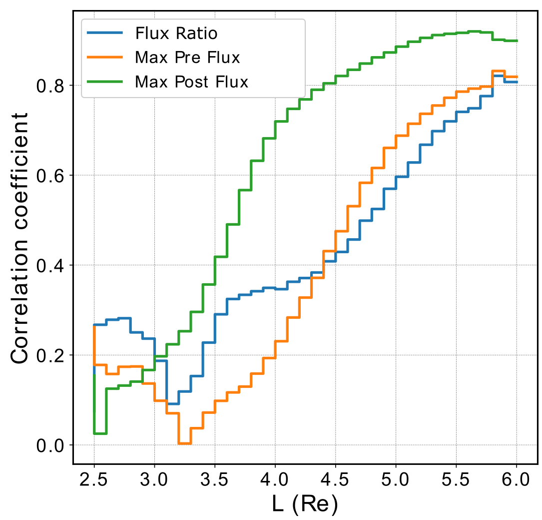

Figure 5. Correlation coefficients of GOES fluxes versus Van Allen Probes at different $L-$shells for flux ratio (blue line), maximum flux post-event $t > 0$ (green line) and maximum flux pre-event $t < 0$.

Examining the correlation of post-to-pre flux ratios we observe a peak of $R = 0.8$ at $L = 5.8$ and a continuous near-linear decrease down to $R = 0.4$ at $L = 4.5$. Then, the correlation continues decreasing but at a slower rate down to $L = 3.5$ where it significantly drops again. The increase in correlation for $L < 3.1$ is yet another indication of how unaffected that part of the outer belt is for most of the enhancement events studied. Of course, correlation of fluxes for $t < 0$ does not depend on the geomagnetic driver resulting in relativistic enhancement event and it probably indicates a natural tendency of the outer radiation belt to remain somewhat coherent in its evolution (Kanekal et al., 2001). Still, a difference in correlation of up to ~ 0.25 in pre or post fluxes shows that geomagnetic activity results in a heavily organized outer belt. Recently Baker et al. (2019) calculated correlations coefficients of daily average fluxes between the Van Allen Probes and GOES data for most of the mission lifetime and found that fluxes are generally correlated to a high degree the closer they are. Still, it is noteworthy that there is a significant difference in the correlation between fluxes for $t < 0$ and for $t > 0$ that indicate that it is more likely to have better predictions capabilities for the outer belt if data from GOES satellites is used as a proxy once a REE is initiated.

By studying the occurrence rate of enhancement events as a function of $L-$shell and by calculating the flux correlations between GEO and different $L-$shells, we show that prediction of events should be possible and relatively simple for $L > 5.0$, and most likely remain very accurate for $L > 4.5$. We also know that relativistic electron events at GEO can be predicted with a fairly high degree of confidence when solar wind and magnetospheric conditions are known by using simple models (O'Brien et al., 2001; Lyons et al., 2009; Lyatsky & Khazanov, 2008; Kim et al., 2015; Pinto et al., 2018) to indicate that an enhancement is likely to occur or with more complex models that will predict the maximum flux levels (Baker et al., 1990; X. Li et al., 2001; Simms et al., 2014, 2016) facilitating a simple prediction mechanism for fluxes across the outer belt for $L > 4.5$. For lower $L-$shells, it may be possible to improve the correlations and, possibly, our degree of predictability if we improve our understanding of the response and occurrence of enhancements by accounting for geomagnetic activity or solar wind parameters.

5 Response to geomagnetic indices

It is well known that geomagnetic indices are useful at characterizing and sometimes predicting the response of the outer radiation belt, and so the most commonly used indices, SYM-H, Kp and AE are studied to determine if they improve the potential for prediction of the response of the belt during REE events at GEO. SYM-H minimum index (or D_{st}) is reflective of the ring current strength and is known to determine fairly well the location of peak electron fluxes in the outer radiation belt following geomagnetic storms (Zhao & Li, 2013; Tverskaya et al., 2003; Moya et al., 2017). The AE index is indicative of substorm particle injections into the inner magnetosphere and is considered relevant for the occurrence of REE events at GEO (Kim et al., 2015; Pinto et al., 2018; Hajra et al., 2015; Antonova et al., 2018; L. Y. Li et al., 2009; Borovsky, 2017) and Kp index indicative of general magnetospheric convection and is regularly used in different forecasting models (e.g. NOAA).

To understand the response of the outer radiation belt to geomagnetic activity as reflected in different geomagnetic indices, we separate the events into 3 groups according to their intensity and describe how those groups of events differentiate from each other. For SYM-H index, we have separated our 60 events into three different groups of roughly the same size according to their minimum SYM-H value within $-24 < t < 24$ hrs. This separation results in thresholds of min(SYM-H) > -48 nT for weak or no storms (20 events), min(SYM-H) < -70 nT for strong storms (18 events). The group of min(SYM-H) in between those two quantities is referred to as the moderate storm group (18 events). For the AE index, we have selected the three groups using thresholds of daily averaged AE index (for the first day of enhancement) of AE $<$ 325 nT (18 events) which will be named “low AE”, 325 $\leq$ AE $\leq$ 430 nT (20 events) which we will refer to as “moderate AE” and AE $>$ 430 nT (22 events) “strong AE”. It is important to mention that compared to quiet times, all these events are actually “strong AE” and our sub-division only makes sense with that understanding in mind. For the Kp index the separation is considered weak for Kp ≤ 4.7, moderate for $5.0 \leq$ Kp < 5.7 and strong for Kp≥ 5.7.

Figure 6 shows a superposed epoch analysis of all events when divided according to their SYM-H minimum value within a day of $t = 0$ (left) or according to their daily average AE index strength for the first day of enhancement $0 < t < 24$ hrs. (right). Similar figures for Kp index and for all events combined are available in the supporting information. Separation according to a particular geomagnetic results in partial separation of other indices as they present some degree of correlation. For example when separating according to min(SYM-H), the events with the strongest drops also have the highest AE indices during the period of enhancement. Similarly, when sorting by the AE indices, increasing AE intensity also results in more pronounced decreases in SYM-H. Nevertheless, we can still get relevant information from this sorting for singular parameters. Possibly the most relevant information is that minimum SYM-H does not discriminate the statistical evolution of fluxes at geostationary orbit. It can be seen in panel 6(a) that all groups present a very similar temporal evolution at GEO with very similar median

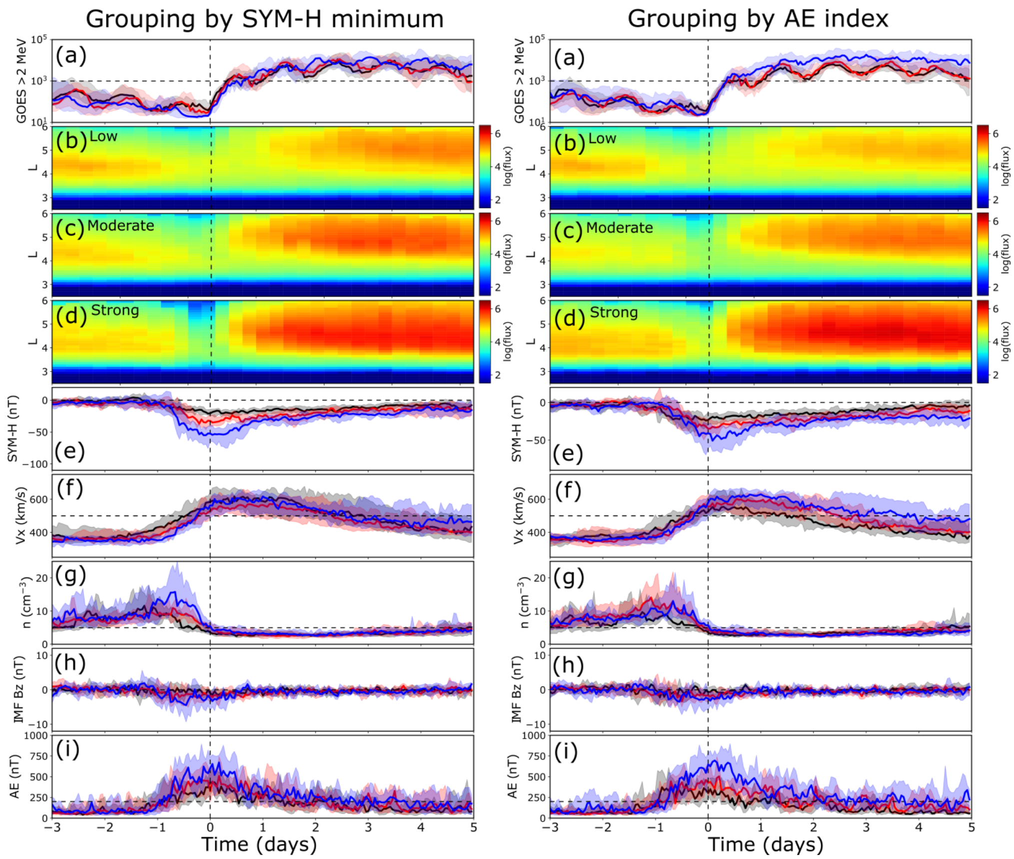

Figure 6. Superposed Epoch Analysis of all events separated according to their SYM-H minimum values (left) and to their averaged AE index (right). From top to bottom (a) GOES $>$ 2 MeV fluxes (e) SYM-H index (f) Solar Wind Speed (g) Solar wind proton density (h) IMF Bz (h) AE index. Solid lines represent median values and the envelopes represent the quartile distributions. Black color is used for weak index group, red for the moderate index group and blue for the strong index group. Van Allen probes$E = 2.1$ MeV flux distribution (median) are shown in panels (b) weak (c) moderate and (d) strong.

values, regardless of that group they are in. In contrast, AE index does a somewhat better job at discriminating the final flux values at GEO based on this group separation. Of course, both minimum SYM-H and AE index separation are significantly better in describing the outer belt response at lower $L-$shell as seen from the Van Allen Probes perspective. Fluxes with a low minimum SYM-H index drop or the lowest AE index take more time reaching enhanced levels and they develop predominantly at high L-shells (panel 6(b). Strong SYM-H drops and the strongest AE index groups develop enhancement across the belt significantly faster and over a wider range of L-shells, with peaks in flux being higher in value and developed at lower $L-$shells compared to the other groups. The top 4 panels in each column of Figure 6 show the essential point of this study, namely that similar enhancements of relativistic electron fluxes at GEO can result in vastly different responses at lower $L-$shells, including the heart of the radiation belts. As a result, studies that only focus on electron fluxes at GEO as a proxy for the entire outer radiation belt and draw conclusions about the radiation belt dynamics from just this one location can be misleading or sometimes simply wrong, as evidenced by the range of responses shown in panels 2-4 from the top. Fortunately, it appears that even a single geomagnetic index combined with fluxes at GEO can significantly improve the predictability of the outer radiation belt at regions interior to GEO.

Figure 7 shows the distribution of maximum electron fluxes before $t = 0$ (a) post $t = 0$ (b) and the post-to-pre flux ratios (c) for all three different groups. Colored dots represent each group; black for the lowest values group, red for the moderate values group and blue for the strong values group. Colored envelopes represent their respective quartile distributions. Figure 7(a) indicates a lack of intense pre-event fluxes on the belt favoring a particular group of SYM-H minimum, and that therefore post flux and ratio should offer some valuable information. Figure 7(b) quantifies what Figure 6 clearly shows, that being for $L > 5.5$ the SYM-H minimum has little impact of the resulting maximum fluxes whereas it plays a very important role in the region $3.5 < L < 5$. It can also be appreciated how even statistically the peaks in flux move inward as the SYM-H minimum decreases. Figure 7(c) also offers some of that information as it is clear that the ratio has a very strong dependence with SYM-H in the region $3.5 < L < 5.0$.

Figure 7(d-i) present the corresponding distributions when events are separated by the magnitude of the daily averaged AE index (d-f) calculated for the first day after $t = 0$. Figure 7(d) shows that although the distributions seem to be relatively similar to each other, they are not identical and the moderate AE group has a slightly lower median in the region $3.7 < L < 5$. We do not anticipate that a pre-conditioning exists here, but the difference may need to be considered when discussing ratios. Figure 7(e) shows extremely clearly separated distributions for all $L > 3$ when daily average AE is larger than 430 nT and for all $L > 4$ for all three groups. It is well known that AE plays an important role in enhancement events at GEO, as it correlates with the amount of energetic electrons that can be injected from the tail through dipolarizations, and even directly injecting MeV electrons well inside the GEO orbit (Dai et al., 2014, 2015; Kanekal

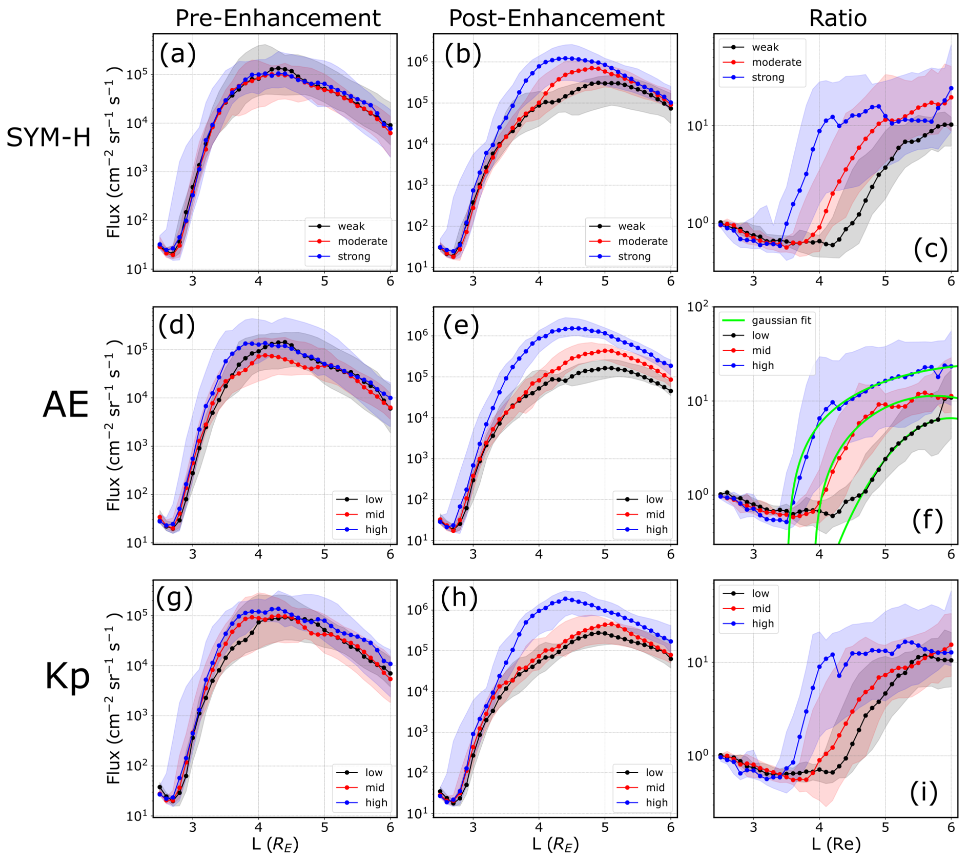

Figure 7. (a) Distribution of maximum fluxes for $t < 0$ when separated in three different groups according to their SYM-H minimum values. Black corresponds to weak (or no) storm, red corresponds to moderate storms and blue corresponds to strong storms. Dotted lines corresponds to the median of each distribution and the colored envelopes to the upper and lower quartiles. (b) Same as in (a) but showing maximum fluxes for $t > 0$. (c) Same as in (a) but for the ratio of change in fluxes. (d-f) Same as in (a-c) but when separating by daily average AE index during the first day after $t = 0$. (g-i) Same as in (a-c) but when separating by maximum Kp index. Green lines in panel (f) correspond to the best Gaussian fit for each of the median curves.

et al., 2016; Tang et al., 2016). It is remarkably how well it differentiates post enhancement fluxes at low L-shells. Figure 7(f) shows the ratio of change between maximum post-to-pre fluxes and again the separation is very clear from one group to the other. Given that AE index presents the most clear separation, we fit each distribution to a Gaussian of the form

$$R = A \exp\left(\frac{(L - L_0)^2}{\sigma}\right) + c$$

where the parameters A, L_0, σ and c have been determined numerically by minimizing the sum of the squared residuals. Table 5 shows the values that provide the best Gaussian fits for all three groups. Although far from perfect, as a first approach to the problem it at least indicates that the response of the radiation belt presents a coherent response that increases, widens in L-shell extent, and moves inward as AE index increases.

Table 1. Gaussian fit coefficients for post-to-pre flux ratios as a function of AE intensity

	A	L_0	σ	c
Lowest AE	6.62	5.98	0.98	-0.05
Mid AE	16.8	5.75	3.08	-5.50
Largest AE	55.9	6.70	17.66	-31.2

Figure 7(g-i) show the distributions for Kp index. Interestingly, Kp index shows little differences in the two lowest groups, which behave similarly in terms of maximum post-fluxes and ratio of enhancement, but for events with $Kp > 5.7$ there is a huge difference in their response through the outer belt. Kp at GEO does show some minor differences across the groups, with the highest Kp events exhibiting a slightly larger statistical increase relative to the other two groups (see supporting information), and that difference can be appreciated down to $L = 5$. However, events with high Kp show a significant difference in the region $3.5 < L < 5.0$ compared to the other two groups, again showing that this particular parameter can be of utility when trying to estimate the fluxes across the radiation belt based on information from GEO. Since Kp and Ap are related to each other, this result is consistent with the findings of Mourenas et al. (2019) who showed that elevated integrated Ap results in high peaks of $E = 2.1$ MeV across the outer belt.

6 Discussion and Conclusions

In our study, we identified 60 relativistic electron enhancement events that were observed at geostationary orbit between 01 September of 2012 and 31 December 2017 using data available from GOES 15 > 2 MeV electrons and the criteria previously established in Pinto et al. (2018). By comparing against simultaneous data available from the Van Allen Probes ECT-REPT (Baker et al., 2013) instrument we studied the response of the $E = 2.1$ MeV electron channel during those 60 REE events.

We have found that despite all events starting off as enhancements in the external part of the outer belt (by definition), the occurrence rate (that is the percentage of events that results in enhancement) decreases significantly for $L < 5.0$ and that some enhancement events can actually result in a depletion of fluxes for $L < 4.6$. Those depletion rates are generally slow and they tend to peak at $L = 4.0$ which may be an indication of a local loss mechanism. The most general behavior is that as L decreases further, the post-to-pre flux ratio gets closer to unity, indicating that the penetration of the enhancement event is always limited to some extent, such that almost no enhancement occurs below $L = 3.0$.

By studying the correlation between flux enhancements at geostationary orbit with contemporaneous fluxes provided by the Van Allen Probes as a function of L, we find that maximum post event fluxes present a very strong correlation between these two regions. Recently, Baker et al. (2019) showed that the correlation coefficient between GEO and different $L-$shells is generally high for any day, and that can be seen by the fact that even pre-enhancement fluxes are relatively well correlated for $L > 4.5$. However, post-enhancement event fluxes present a much larger correlation down to $L = 4.0$ indicating that predictions of the response of the belt up to that point should be relatively accurate, but only at post-enhancement times.

We have also studied the response of the outer radiation belt when we separate the events according to the strength of certain geomagnetic indices, in particular SYM-H, AE and Kp, since they are all known to be effective at modulating the response of the outer belt. We have found so far that all three studied parameters are useful in describing part of the response of the outer belt in terms of ratio of enhancement, peak of the fluxes and maximum post flux values and location. We also examined several solar wind parameters (solar wind speed, solar wind proton density, solar wind dynamic pressure, IMF southward directed B_z and time of southward directed B_z) attempting to separate them in three groups as we did with geomagnetic indices. We have included those results in the supporting information, because the solar wind parameters leading to enhancement events are strongly correlated with geomagnetic indices. Thus, the results are somewhat redundant with what we have discussed already.

This study has attempted to quantify what other studies have suggested, that fluxes at GEO can be used as a proxy for the fluxes throughout the whole outer radiation belt. In a first step, we have demonstrated that it is possible to use GEO for the occurrence of enhancement events and enhanced fluxes with high accuracy for $L > 5$ and with moderate accuracy for $L > 4$. While reconstructing the fluxes of the radiation belt in real time using proxy data seems unlikely, and it is necessary to have real time in-situ measurements for increased prediction potential, the use of GEO. Although not discussed here, it is possible that by adding GPS and low altitude measurements results in an improved description of the system, in particular at lower ($L < 4$) radial distances and therefore improved predictions of fluxes throughout the outer radiation belt.

Acknowledgments

VAP thanks the support of Becas Chile program. VAP and JB would like to acknowledge support by RBSP-ECT and EMFISIS funding provided by JHU/APL contract No. 967399 and 921647 under NASAs prime contract No. NAS5-01072, as well as NASA grants and NNX14AI18G. P.S.M. is grateful for the support of CONICyT Chile through FONDECyT Grant No. 1191351. We acknowledge NASA/GSFCs Space Physics Data Facilitys OMNIWeb and CDAWeb services and OMNI data for providing solar wind data and magnetospheric indices (https://cdaweb.sci.gsfc.nasa.gov/) and the Van Allen Probes ECT-REPT team. REPT data was obtained from SODC (https://www.rbsp-ect.lanl.gov/). This paper is dedicated to the memory of the recently deceased Prof. Richard M. Thorne for his pioneering work in the field of radiation belt dynamics.

References

Anderson, B. R., Millan, R. M., Reeves, G. D., & Friedel, R. H. W. (2015). Acceleration and loss of relativistic electrons during small geomagnetic storms. *Geophysical Research Letters*, *42*(23), 10,113–10,119. doi: 10.1002/2015GL066376

Antonova, E. E., Stepanova, M. V., Moya, P. S., Pinto, V. A., Vovchenko, V. V., Ovchinnikov, I. L., & Sotnikov, N. V. (2018). Processes in auroral oval and outer electron radiation belt. *Earth, Planets and Space*, *70*(1). doi: 10.1186/s40623-018-0898-1

Baker, D. N. (2000). The occurrence of operational anomalies in spacecraft and their relationship to space weather. *IEEE Transactions on Plasma Science*, *28*(6), 2007–2016.

Baker, D. N., Blake, J. B., Klebesadel, R. W., & Higbie, P. R. (1986). Highly relativistic electrons in the Earth's outer magnetosphere: 1. Lifetimes and temporal history 1979–1984. *Journal of Geophysical Research*, *91*(A4), 4265. doi: 10.1029/JA091iA04p04265

Baker, D. N., Kanekal, S. G., Hoxie, V. C., Batiste, S., Bolton, M., Li, X., … Friedel, R. (2013). The Relativistic Electron-Proton Telescope (REPT) Instrument on Board the Radiation Belt Storm Probes (RBSP) Spacecraft: Characterization of Earth's Radiation Belt High-Energy Particle Populations. *Space Science Reviews*, *179*(1-4), 337–381. doi: 10.1007/s11214-012-9950-9

Baker, D. N., McPherron, R. L., Cayton, T. E., & Klebesadel, R. W. (1990). Linear prediction filter analysis of relativistic electron properties at 6.6 R_E. *Journal of Geophysical Research*, *95*(A9), 15133. doi: 10.1029/JA095iA09p15133

Baker, D. N., Zhao, H., Li, X., Kanekal, S. G., Jaynes, A. N., Kress, B. T., … Hoxie, V. (2019). Comparison of Van Allen Probes Energetic Electron Data With Corresponding GOES-15 Measurements: 2012–2018. *Journal of Geophysical Research: Space Physics*, *124*(12), 9924–9942. doi: 10.1029/2019JA027331

Balikhin, M. A., Boynton, R. J., Walker, S. N., Borovsky, J. E., Billings, S. A., & Wei, H. L. (2011). Using the NARMAX approach to model the evolution of energetic electrons fluxes at geostationary orbit. *Geophysical Research Letters*, *38*(18), n/a-n/a. doi: 10.1029/2011GL048980

Bingham, S. T., Mouikis, C. G., Kistler, L. M., Boyd, A. J., Paulson, K., Farrugia, C. J., … Kletzing, C. (2018). The outer radiation belt response to the storm time development of seed electrons and chorus wave activity during CME and CIR storms. *Journal of Geophysical Research: Space Physics*. doi: 10.1029/2018JA025963

Blum, L. W., & Breneman, A. W. (2019). Observations of radiation belt losses due to cyclotron wave-particle interactions. In *The Dynamic Loss of Earth's Radiation Belts* (pp. 49–98). Elsevier. doi: 10.1016/B978-0-12-813371-2.00003-2

Borovsky, J. E. (2017). Time-Integral Correlations of Multiple Variables With the Relativistic-Electron Flux at Geosynchronous Orbit: The Strong Roles of Substorm-Injected Electrons and the Ion Plasma Sheet: Time-Integral Radiation Belt Correlation. *J. Geophys. Res. Space Physics*, *122*(12), 11,961–11,990. doi: 10.1002/2017JA024476

Borovsky, J. E., & Denton, M. H. (2006). Differences between CME-driven storms and CIR-driven storms. *Journal of Geophysical Research*, *111*(A7). doi: 10.1029/2005JA011447

Borovsky, J. E., & Denton, M. H. (2010). Magnetic field at geosynchronous orbit during high-speed stream-driven storms: Connections to the solar wind, the plasma sheet, and the outer electron radiation belt. *Journal of Geophysical Research: Space Physics*, *115*(A8), n/a-n/a. doi: 10.1029/2009JA015116

Bortnik, J., Thorne, R. M., O'Brien, T. P., Green, J. C., Strangeway, R. J., Shprits, Y. Y., & Baker, D. N. (2006). Observation of two distinct, rapid loss mechanisms during the 20 November 2003 radiation belt dropout event. *Journal of Geophysical Research*, *111*(A12). doi: 10.1029/2006JA011802

Boynton, R. J., Balikhin, M. A., & Billings, S. A. (2015). Online NARMAX model for electron fluxes at GEO. *Annales Geophysicae*, *33*(3), 405–411. doi: 10.5194/angeo-33-405-2015

Dai, L., Wang, C., Duan, S., He, Z., Wygant, J. R., Cattell, C. A., ... Tang, X. (2015). Near-Earth injection of MeV electrons associated with intense dipolarization electric fields: Van Allen Probes observations: SUBSTORM INJECTIONS OF MEV ELECTRONS. *Geophysical Research Letters*, *42*(15), 6170–6179. doi: 10.1002/2015GL064955

Dai, L., Wygant, J. R., Cattell, C. A., Thaller, S., Kersten, K., Breneman, A., ... Tao, X. (2014). Evidence for injection of relativistic electrons into the Earth's outer radiation belt via intense substorm electric fields. *Geophysical Research Letters*, *41*(4), 1133–1141. doi: 10.1002/2014GL059228

Denton, M. H., & Borovsky, J. E. (2012). Magnetosphere response to high-speed solar wind streams: A comparison of weak and strong driving and the importance of extended periods of fast solar wind. *J. Geophys. Res.*, *117*(A9), n/a-n/a. doi: 10.1029/2011JA017124

Gonzalez, W. D., Joselyn, J. A., Kamide, Y., Kroehl, H. W., Rostoker, G., Tsurutani, B. T., & Vasyliunas, V. M. (1994). What is a geomagnetic storm? *Journal of Geophysical Research*, *99*(A4), 5771. doi: 10.1029/93JA02867

Hajra, R., Tsurutani, B. T., Echer, E., Gonzalez, W. D., & Santolik, O. (2015).

Relativistic (E > 0.6, > 2.0, AND > 4.0 MeV) Electron Acceleration at Geosynchronous Orbit During High-Intensity, Long-Duration, Continuous AE Activity (HILDCAA) Events. *The Astrophysical Journal*, *799*(1), 39. doi: 10.1088/0004-637X/799/1/39

Iles, R. H. A., Fazakerley, A. N., Johnstone, A. D., Meredith, N. P., & Bühler, P. (2002). The relativistic electron response in the outer radiation belt during magnetic storms. *Annales Geophysicae*, *20*, 957–965.

Jaynes, A. N., Baker, D. N., Singer, H. J., Rodriguez, J. V., Loto'aniu, T. M., Ali, A. F., … Reeves, G. D. (2015). Source and seed populations for relativistic electrons: Their roles in radiation belt changes. *Journal of Geophysical Research: Space Physics*, *120*(9), 7240–7254. doi: 10.1002/2015JA021234

Kanekal, S. G., Baker, D. N., & Blake, J. B. (2001). Multisatellite measurements of relativistic electrons: Global coherence. *Journal of Geophysical Research: Space Physics*, *106*(A12), 29721–29732. doi: 10.1029/2001JA000070

Kanekal, S. G., Baker, D. N., Fennell, J. F., Jones, A., Schiller, Q., Richardson, I. G., … Wygant, J. R. (2016). Prompt acceleration of magnetospheric electrons to ultrarelativistic energies by the 17 March 2015 interplanetary shock. *Journal of Geophysical Research: Space Physics*, *121*(8), 7622–7635. doi: 10.1002/2016JA022596

Katsavrias, C., Daglis, I. A., & Li, W. (2019). On the Statistics of Acceleration and Loss of Relativistic Electrons in the Outer Radiation Belt: A Superposed Epoch Analysis. *J. Geophys. Res. Space Physics*, 2019JA026569. doi: 10.1029/2019JA026569

Kim, H.-J., & Chan, A. A. (1997). Fully adiabatic changes in storm time relativistic electron fluxes. *Journal of Geophysical Research: Space Physics*, *102*(A10), 22107–22116. doi: 10.1029/97JA01814

Kim, H.-J., Kim, K. C., Lee, D.-Y., & Rostoker, G. (2006). Origin of geosynchronous relativistic electron events. *Journal of Geophysical Research*, *111*(A3). doi: 10.1029/2005JA011469

Kim, H.-J., Lyons, L., Pinto, V., Wang, C.-P., & Kim, K.-C. (2015). Revisit of relationship between geosynchronous relativistic electron enhancements and magnetic storms. *Geophysical Research Letters*, *42*(15), 6155–6161. doi: 10.1002/2015GL065192

Li, L. Y., Cao, J. B., Zhou, G. C., & Li, X. (2009). Statistical roles of storms and substorms in changing the entire outer zone relativistic electron population. *Journal of Geophysical Research: Space Physics*, *114*(A12), n/a-n/a. doi: 10.1029/2009JA014333

Li, W., Thorne, R. M., Bortnik, J., Baker, D. N., Reeves, G. D., Kanekal, S. G., … Green, J. C. (2015). Solar wind conditions leading to efficient radiation belt electron acceleration: A superposed epoch analysis. *Geophysical Research Letters*, *42*(17), 6906–6915. doi: 10.1002/2015GL065342

Li, X., Baker, D. N., Teremin, M., Cayton, T. E., Reeves, G. D., Selesnick, R. S., … Singer, H. J. (1999). Rapid enchancements of relativistic electrons deep in the magnetosphere during the May 15, 1997, magnetic storm. *J. Geophys. Res.*, *104*(A3), 4467–4476. doi: 10.1029/1998JA900092

Li, X., Temerin, M., Baker, D. N., Reeves, G. D., & Larson, D. (2001). Quantitative prediction of radiation belt electrons at geostationary orbit based on solar wind measurements. *Geophysical Research Letters*, *28*(9), 1887–1890.

Lyatsky, W., & Khazanov, G. V. (2008). Effect of solar wind density on relativistic electrons at geosynchronous orbit. *Geophysical Research Letters*, *35*(3). doi: 10.1029/2007GL032524

Lyons, L., Lee, D.-Y., Kim, H.-J., Hwang, J., Thorne, R., Horne, R., & Smith, A. (2009). Solar-wind–magnetosphere coupling, including relativistic electron energization, during high-speed streams. *Journal of Atmospheric and Solar-Terrestrial Physics*, *71*(10-11), 1059–1072. doi: 10.1016/j.jastp.2008.04.016

Mauk, B. H., Fox, N. J., Kanekal, S. G., Kessel, R. L., Sibeck, D. G., & Ukhorskiy, A. (2013). Science Objectives and Rationale for the Radiation Belt Storm Probes Mission. *Space Science Reviews*, *179*(1-4), 3–27. doi: 10.1007/s11214-012-9908-y

Millan, R., & Thorne, R. (2007). Review of radiation belt relativistic electron losses. *Journal of Atmospheric and Solar-Terrestrial Physics*, *69*(3), 362–377. doi: 10.1016/j.jastp.2006.06.019

Mourenas, D., Artemyev, A. V., Ma, Q., Agapitov, O. V., & Li, W. (2016). Fast dropouts of multi-MeV electrons due to combined effects of EMIC and whistler mode waves. *Geophysical Research Letters*, *43*(9), 4155–4163. doi: 10.1002/2016GL068921

Mourenas, D., Artemyev, A. V., & Zhang, X.-J. (2019). Impact of significant time-integrated geomagnetic activity on 2 MeV electron flux. *J. Geophys. Res. Space Physics*, 2019JA026659. doi: 10.1029/2019JA026659

Moya, P. S., Pinto, V. A., Sibeck, D. G., Kanekal, S. G., & Baker, D. N. (2017). On the Effect of Geomagnetic Storms on Relativistic Electrons in the Outer Radiation Belt: Van Allen Probes Observations. *Journal of Geophysical Research: Space Physics*, *122*(11), 11,100–11,108. doi: 10.1002/2017JA024735

Murphy, K. R., Watt, C. E. J., Mann, I. R., Jonathan Rae, I., Sibeck, D. G., Boyd, A. J., ... Fennell, J. (2018). The Global Statistical Response of the Outer Radiation Belt During Geomagnetic Storms. *Geophysical Research Letters*, *45*(9), 3783–3792. doi: 10.1002/2017GL076674

O'Brien, T. P., McPherron, R. L., Sornette, D., Reeves, G. D., Friedel, R., & Singer, H. J. (2001). Which magnetic storms produce relativistic electrons at geosynchronous orbit? *Journal of Geophysical Research: Space Physics*, *106*(A8), 15533–15544. doi: 10.1029/2001JA000052

Pandya, M., Bhaskara, V., Ebihara, Y., Kanekal, S. G., & Baker, D. N. (2019). Variation of Radiation Belt Electron Flux During CME- and CIR-Driven Geomagnetic Storms: Van Allen Probes Observations. *J. Geophys. Res. Space Physics*, 2019JA026771. doi: 10.1029/2019JA026771

Paulikas, G., & Blake, J. (1979). Effects of the Solar Wind on Magnetospheric Dynamics: Energetic Electrons at the Synchronous Orbit. In W. P. Olson (Ed.), *Geophysical Monograph Series* (pp. 180–202). Washington, D. C.: American Geophysical Union. doi: 10.1029/GM021p0180

Pinto, V. A., Kim, H.-J., Lyons, L. R., & Bortnik, J. (2018). Interplanetary Parameters Leading to Relativistic Electron Enhancement and Persistent Depletion Events at Geosynchronous Orbit and Potential for Prediction. *Journal of Geophysical Research: Space Physics*, *123*(2), 1134–1145. doi: 10.1002/2017JA024902

Reeves, G. D. (1998). Relativistic electrons and magnetic storms: 1992-1995. *Geophysical Research Letters*, *25*(11), 1817–1820. doi: 10.1029/98GL01398

Reeves, G. D., McAdams, K. L., Friedel, R. H. W., & O'Brien, T. P. (2003). Acceleration and loss of relativistic electrons during geomagnetic storms. *Geophysical Research Letters*, *30*(10), n/a-n/a. doi: 10.1029/2002GL016513

Reeves, G. D., Morley, S. K., Friedel, R. H. W., Henderson, M. G., Cayton, T. E., Cunningham, G., … Thomsen, D. (2011). On the relationship between relativistic electron flux and solar wind velocity: Paulikas and Blake revisited. *Journal of Geophysical Research: Space Physics*, *116*(A2), n/a-n/a. doi: 10.1029/2010JA015735

Rodriguez, J. V., Krosschell, J. C., & Green, J. C. (2014). Intercalibration of GOES 8-15 solar proton detectors. *Space Weather*, *12*(1), 92–109. doi: 10.1002/2013SW000996

Schiller, Q., Li, X., Blum, L., Tu, W., Turner, D. L., & Blake, J. B. (2014). A non-storm time enhancement of relativistic electrons in the outer radiation belt. *Geophysical Research Letters*, *41*(1), 7–12. doi: 10.1002/2013GL058485

Shen, X.-C., Hudson, M. K., Jaynes, A. N., Shi, Q., Tian, A., Claudepierre, S. G., … Sun, W.-J. (2017). Statistical study of the storm time radiation belt evolution during Van Allen Probes era: CME- versus CIR-driven storms. *Journal of Geophysical Research: Space Physics*, *122*(8), 8327–8339. doi: 10.1002/2017JA024100

Simms, L. E., Engebretson, M. J., Pilipenko, V., Reeves, G. D., & Clilverd, M. (2016). Empirical predictive models of daily relativistic electron flux at geostationary orbit: Multiple regression analysis. *Journal of Geophysical Research: Space Physics*, *121*(4), 3181–3197. doi: 10.1002/2016JA022414

Simms, L. E., Pilipenko, V., Engebretson, M. J., Reeves, G. D., Smith, A. J., & Clilverd, M. (2014). Prediction of relativistic electron flux at geostationary orbit following storms: Multiple regression analysis. *Journal of Geophysical Research: Space Physics*, *119*(9), 7297–7318. doi: 10.1002/2014JA019955

Spence, H. E., Reeves, G. D., Baker, D. N., Blake, J. B., Bolton, M., Bourdarie, S., … Thorne, R. M. (2013). Science Goals and Overview of the Radiation Belt Storm Probes (RBSP) Energetic Particle, Composition, and Thermal Plasma (ECT) Suite on NASA's Van Allen Probes Mission. *Space Science Reviews*, *179*(1-4), 311–336. doi: 10.1007/s11214-013-0007-5

Su, Z., Xiao, F., Zheng, H., He, Z., Zhu, H., Zhang, M., … Baker, D. N. (2014). Nonstorm time dynamics of electron radiation belts observed by the Van Allen Probes. *Geophysical Research Letters*, *41*(2), 229–235. doi: 10.1002/2013GL058912

Tang, C. L., Wang, Y. X., Ni, B., Su, Z. P., Reeves, G. D., Zhang, J.-C., ... Blake, J. B. (2017). The effects of magnetospheric processes on relativistic electron dynamics in the Earth's outer radiation belt. *J. Geophys. Res. Space Physics*, *122*(10), 9952–9968. doi: 10.1002/2017JA024407

Tang, C. L., Zhang, J.-C., Reeves, G. D., Su, Z. P., Baker, D. N., Spence, H. E., ... Wygant, J. R. (2016). Prompt enhancement of the Earth's outer radiation belt due to substorm electron injections. *Journal of Geophysical Research: Space Physics*, *121*(12), 11,826–11,838. doi: 10.1002/2016JA023550

Thorne, R. M. (2010). Radiation belt dynamics: The importance of wave-particle interactions. *Geophysical Research Letters*, *37*(22), n/a-n/a. doi: 10.1029/2010GL044990

Thorne, R. M., Li, W., Ni, B., Ma, Q., Bortnik, J., Chen, L., ... Kanekal, S. G. (2013). Rapid local acceleration of relativistic radiation-belt electrons by magnetospheric chorus. *Nature*, *504*(7480), 411–414. doi: 10.1038/nature12889

Turner, D. L., Kilpua, E. K. J., Hietala, H., Claudepierre, S. G., O'Brien, T. P., Fennell, J. F., ... Reeves, G. D. (2019). The response of Earth's electron radiation belts to geomagnetic storms: Statistics from the Van Allen Probes era including effects from different storm drivers. *Journal of Geophysical Research: Space Physics*. doi: 10.1029/2018JA026066

Turner, D. L., & Li, X. (2008). Quantitative forecast of relativistic electron flux at geosynchronous orbit based on low-energy electron flux. *Space Weather*, *6*(5), n/a-n/a. doi: 10.1029/2007SW000354

Turner, D. L., O'Brien, T. P., Fennell, J. F., Claudepierre, S. G., Blake, J. B., Kilpua, E. K. J., & Hietala, H. (2015). The effects of geomagnetic storms on electrons in Earth's radiation belts. *Geophysical Research Letters*, *42*(21), 9176–9184. doi: 10.1002/2015GL064747

Tverskaya, L., Pavlov, N., Blake, J., Selesnick, R., & Fennell, J. (2003). Predicting the L-position of the storm-injected relativistic electron belt. *Advances in Space Research*, *31*(4), 1039–1044. doi: 10.1016/S0273-1177(02)00785-8

Wrenn, G. (2009). Chronology of 'killer' electrons: Solar cycles 22 and 23. *Journal of Atmospheric and Solar-Terrestrial Physics*, *71*(10-11), 1210–1218. doi: 10.1016/j.jastp.2008.08.002

Wrenn, G. L., Rodgers, D. J., & Ryden, K. A. (2002). A solar cycle of spacecraft anomalies due to internal charging. *Annales Geophysicae*, *20*(7), 953–956. doi: 10.5194/angeo-20-953-2002

Xiong, Y., Xie, L., Chen, L., Ni, B., Fu, S., & Pu, Z. (2018). The Response of the Energy Content of the Outer Electron Radiation Belt to Geomagnetic Storms. *Journal of Geophysical Research: Space Physics*, *123*(10), 8227–8240. doi: 10.1029/2018JA025475

Xiong, Y., Xie, L., Pu, Z., Fu, S., Chen, L., Ni, B., ... Parks, G. K. (2015). Responses of relativistic electron fluxes in the outer radiation belt to geomagnetic storms. *Journal of Geophysical Research: Space Physics*, *120*(11), 9513–9523. doi: 10.1002/2015JA021440

Yuan, C.-J., & Zong, Q.-G. (2019). The Efficiency of Coronal Mass Ejection With Different IMF Preconditions on the Production of Megaelectronvolt Electron Content in the Outer Radiation Belt. *J. Geophys. Res. Space Physics*, *124*(5), 3222–3235. doi: 10.1029/2018JA026263

Zhao, H., Baker, D. N., Li, X., Jaynes, A. N., & Kanekal, S. G. (2019). The effects of geomagnetic storms and solar wind conditions on the ultrarelativistic electron flux enhancements. *Journal of Geophysical Research: Space Physics*. doi: 10.1029/2018JA026257

Zhao, H., & Li, X. (2013). Inward shift of outer radiation belt electrons as a function of *Dst* index and the influence of the solar wind on electron injections into the slot region. *Journal of Geophysical Research: Space Physics*, *118*(2), 756–764. doi: 10.1029/2012JA018179